Rate Effects in Tertiary Micellar Flooding of Bradford Crude Oil

M.H.M. Sayyouh, SPE, Cairo U.
S.M. Farouq Ali, SPE, U. of Alberta
C.D. Stahl, SPE, Pennsylvania State U.

Abstract

Micellar flooding of the tight Pennsylvania oil reservoirs invariably is accompanied by low flood advance rates – on the order of a fraction of 1 ft/D. This investigation, therefore, was devoted to the effect of rate on tertiary oil recovery.

The experiments were conducted in 2- and 4-ft-long Berea sandstone cores at rates as low as 0.10 ft/D. All runs were tertiary in nature. The micellar solutions being used in the field tests in Pennsylvania also were used for this research. The majority of the runs were carried out in horizontally positioned cores (although a few runs used vertical cores) to determine if gravity was a factor in the observed effect.

It was found that oil recovery decreased with a decrease in the flood advance rate up to a point. Thereafter, it showed a small increase with further decrease in rate. This effect has not been reported by other investigators.

The rate effect is discussed and analyzed in terms of the system phase behavior, sulfonate adsorption, dispersion, diffusion, and mobility control. The role of the rate effect on the formation of the stabilized bank also was developed for the experimental conditions involved. The implications of very low rates are discussed in the light of field results.

Introduction

During recent years, much effort has been devoted to investigations of oil displacement by micellar solutions. This process was proposed and described in detail by Gogarty and Tosch[1] and Davis and Jones.[2] An analysis of the mechanism of the process is given by Bleakley.[3] The micellar solutions are composed primarily of a hydrocarbon, water, a surfactant, and a cosurfactant. Micellar flooding involves sequential injection of a micellar slug, a mobility buffer, and drive water.

Since one of the significant characteristics of Pennsylvania oil reservoirs is the low formation permeability, waterflood rates in many of these reservoirs are much less than 1 ft/D. Currently, tertiary micellar floods are being conducted in these reservoirs. Thus, it is important to investigate the recovery behavior of micellar displacement at comparable flow rates. Taber *et al.*[4] observed that at both higher and lower rates the displacement of oil and water by an alcohol was efficient. This was confirmed later by Taber and Meyer.[5] An increase in microemulsion displacement efficiency at high rates was observed by Healy *et al.*[6]

In our previous work,[7] the effect of flood advance rate in micellar/polymer displacement process under a wide variety of conditions was investigated to determine (1) what effect do flow rates have on oil recovery and (2) whether flow rate itself or some other factor, such as gravity segregation, contributes to the observed behavior. Oil recovery was found to be rate dependent under these conditions.

One objective of this work is to analyze the effect of flood advance rates in terms of system phase behavior, sulfonate adsorption, mixing mechanism, and mobility control. Another purpose is to understand the effect of rate on the formation of the stabilized oil/water bank and discuss the implications of very low rates.

Experimental Results Showing Effect of Rate on Tertiary Oil Recovery

An experimental investigation was carried out to study the variation of tertiary oil recovery with rate, using different slug sizes for horizontal and vertical displacements in 4- and 2-ft-long cores. (Material, apparatus, and experimental techniques are described in Appendix A.) Summary of the results is given in Table 1. It is evident that in all cases recovery increased with an increase in slug size. Two different micellar slugs were used. Runs 1 through 29 and 31 through 34 employed the Richburg slug. The

0197-7520/81/0003-7639$00.25

TABLE 1 – SUMMARY OF TERTIARY MICELLAR SOLUTION FLOOD – KELZAN-BUFFER/BRADFORD-CRUDE/BEREA-SANDSTONE CORES

	Core Characteristics				Buffer	Micellar Solution		Initial Tertiary	Fractional Flow of		Tertiary Oil	
Run	Length (ft)	k_a (md)	Position	Rate (ft/D)	Size (% PV)	Size (% PV)	Type	Oil Saturation	Oil/Water Bank	Micellar Recovery (% injected)	Recovery (% injected)	Remarks
1	4	198	horizontal	4.35	25	2.5	Richburg	23.70	0.225	–	28.13	
2	4	332	horizontal	4.35	25	5	Richburg	33.47	– 0.411	43.72	60.72	
3	4	158	horizontal	0.94	25	5	Richburg	35.66	0.319	70.26	43.70	
4	4	137	horizontal	0.94	25	2.5	Richburg	33.10	0.221	1.07	24.47	
5	4	107	horizontal	0.94	25	10	Richburg	32.80	0.382	82.40	64.04	
6	4	323	horizontal	4.35	25	10	Richburg	25.70	0.322	3.79	66.73	
7	4	200	horizontal	0.50	25	2.5	Richburg	27.00	0.242	2.03	28.22	
8	4	220	horizontal	0.50	25	5	Richburg	31.40	0.312	7.64	54.46	
9	4	213	horizontal	0.50	25	10	Richburg	32.35	0.332	4.02	69.75	
10	4	210	horizontal	0.50	25	15	Richburg	33.80	0.351	7.16	71.44	
11	2	138	horizontal	0.20	25	2.5	Richburg	36.00	–	96.26	40.64	
12	2	217	horizontal	0.20	25	5	Richburg	31.80	0.200	25.36	44.44	
13	2	169	horizontal	0.20	25	10	Richburg	27.68	0.214	18.15	61.13	
14	2	239	vertical	0.94	25	10	Richburg	30.74	0.325	86.30	65.16	
15	2	239	vertical	0.94	25	5	Richburg	27.70	0.264	10.17	56.13	
16	2	71	vertical	0.94	25	2.5	Richburg	34.70	0.226	29.95	26.99	
17	2	146	vertical	4.35	25	2.5	Richburg	30.40	0.187	5.83	32.74	
18	2	146	vertical	4.35	25	5	Richburg	30.40	0.356	5.13	58.63	
19	2	146	vertical	4.35	25	10	Richburg	32.00	0.321	5.47	81.33	
20	2	146	horizontal	0.94	25	5	Richburg	32.00	0.380	10.06	52.31	
21	2	145	horizontal	0.94	25	2.5	Richburg	32.65	0.147	23.44	25.05	
22	2	146	horizontal	0.94	25	10	Richburg	31.20	0.318	13.40	64.65	
23	2	125	horizontal	0.50	25	5	Richburg	27.20	0.254	19.23	50.34	
24	2	131	horizontal	0.50	25	15	Richburg	30.20	0.527	1.55	70.53	
25	2	139	horizontal	0.94	25	5	Richburg	30.20	0.242	31.81	46.91	
26	2	125	horizontal	0.10	25	10	Richburg	28.90	0.272	2.63	63.04	
27	2	110	horizontal	0.10	25	5	Richburg	24.40	0.227	23.70	49.68	
28	2	167	horizontal	0.10	25	2.5	Richburg	33.90	0.249	39.41	47.47	
29	2	175	horizontal	4.35	25	10	Richburg	28.00	0.342	0.28	82.45	
30	2	112	horizontal	4.35	25	2.5	Bradford	32.20	0.259	30.36	44.69	
31	2	363	horizontal	1.00	25	10	Richburg	31.30	0.371	28.98	64.50	
32	2	112	horizontal	1.00	25	5	Richburg	37.00	0.378	48.78	48.78	
33	2	79	horizontal	1.00	25	10	Richburg	35.30	0.387	4.48	51.02	decomposed slug
34	2	193	horizontal	1.00	25	5	Richburg	29.30	0.282	4.12	25.43	decomposed slug
35	2	442	horizontal	2.6	25	10	Bradford	37.30	0.409	24.26	67.49	
36	2	105	horizontal	5.2	25	10	Bradford	32.30	0.422	27.46	68.16	
37	2	393	horizontal	0.25	25	10	Bradford	44.50	0.385	16.35	43.50	
38	2	257	horizontal	5.2	25	10	Bradford	31.40	0.310	10.46	68.94	
39	2	–	horizontal	0.5	25	5	Richburg	30.0	0.305	4.41	53.40	decomposed slug
40	2	272	horizontal	5.2	25	10 2	Bradford	34.0	0.355	5.69	76.40	470-ppm Kelzan
41	2	163	horizontal	0.10	25	10	Bradford	32.30	0.347	4.77	56.09	

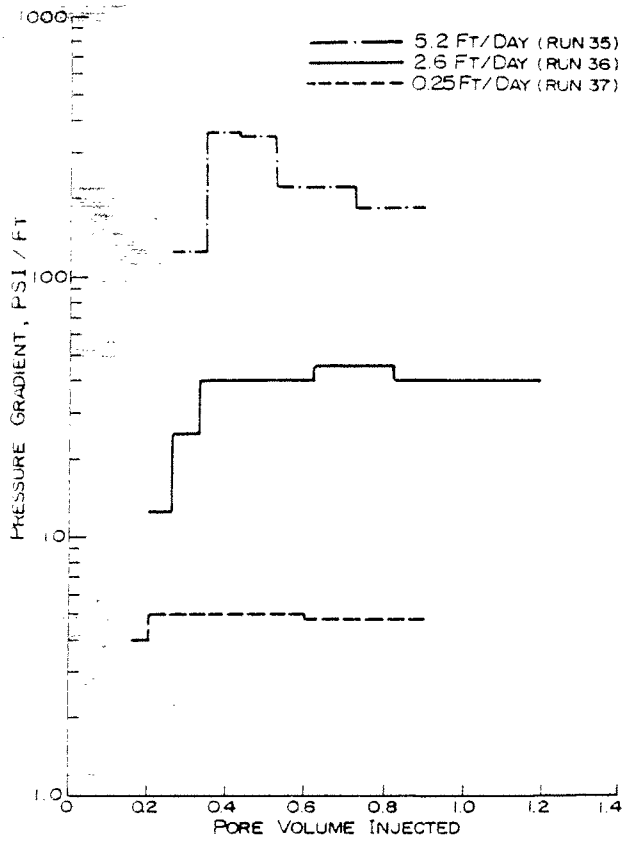

Fig. 6 – Pressure behavior at different injection rates.

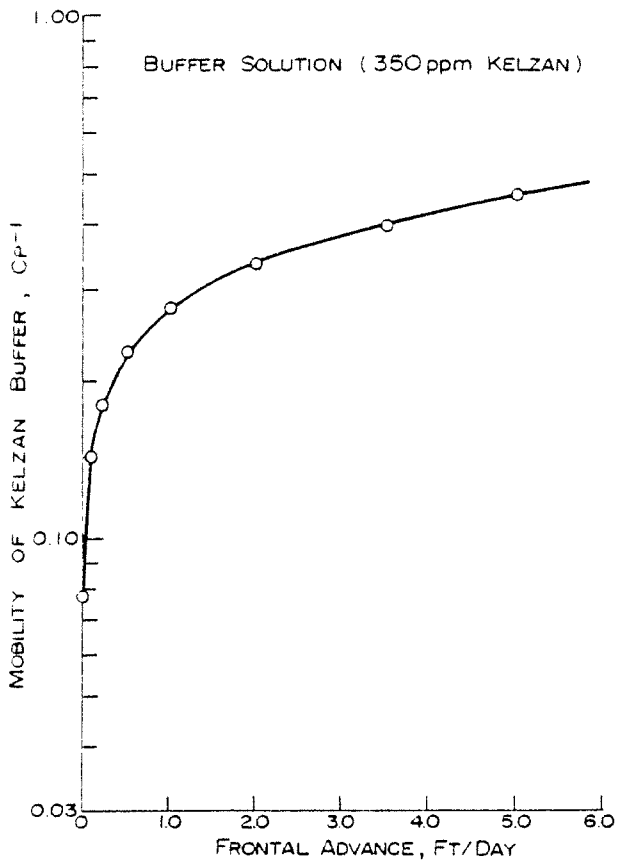

Fig. 8 – Mobility of Kelzan buffer as a function of flood advance rate.

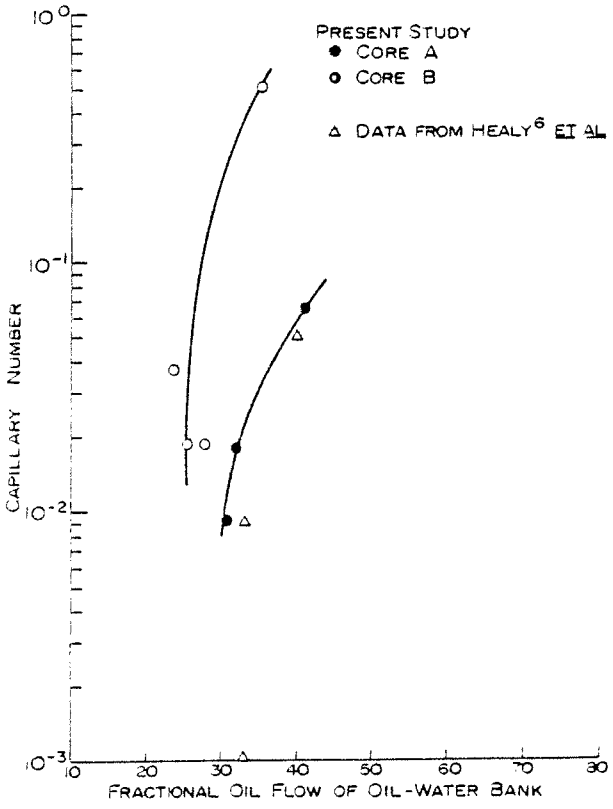

Fig. 7 – Fractional oil flow of oil/water bank as a function of capillary number.

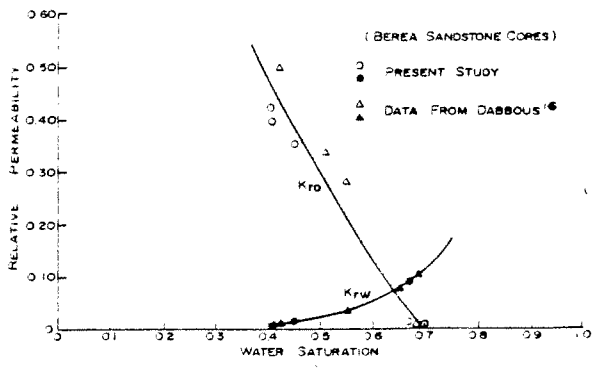

Fig. 9 – Relative permeability curves for Berea sandstone cores.

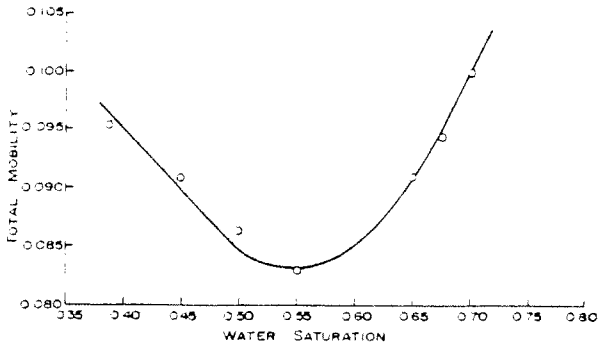

Fig. 10 – Variation of total mobility with water saturation.

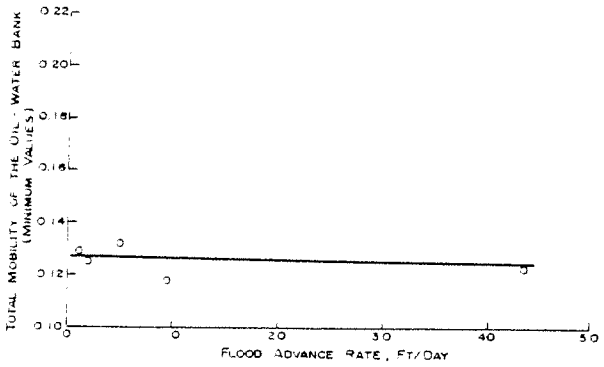

Fig. 11 – Variation of total mobility of stabilized oil/water bank with rate.

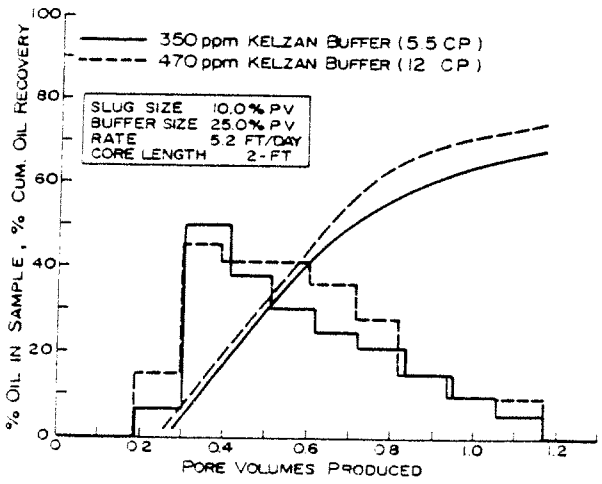

Fig. 12 – Production histories for 10% PV slug and 25% PV Kelzan buffer (350 and 470 ppm) displacements in 2-ft cores at 5.2 ft/D.

total mobility of the oil/water bank and the flood advance rate. This relationship is developed from

$$\lambda_{sob} = \lambda_w (1 - f_{sob})^{-1} \quad \ldots\ldots\ldots\ldots\ldots\ldots (4)$$

Since water is a Newtonian fluid, λ_w is rate independent and Eq. 4 shows the total mobility dependence of fractional flow of the stabilized oil/water bank. Fig. 11 shows that the total mobility* of the oil/water bank is rate independent within the rates used. Chang *et al.*[11] found that the total mobility is rate sensitive at extremely high rates (~140 ft/D)

Two important observations concerning the mobility control mechanism can be made:

1. A decrease in flood advance rates at very low values will lead to a considerable decrease in the mobility of the buffer solution as shown in Fig. 8, whereas the total mobility of the oil/water bank is rate independent as indicated by Fig. 11.

2. The minimum total mobility of the stabilized oil/water bank is established at 0.083 cp^{-1} on the basis of Fig. 10.

Two runs were carried out to study the behavior of oil recovery using 350-ppm (5.5-cp) and 470-ppm (12-cp) Kelzan buffer at 5.2 ft/D. The results indicated that the displacement efficiency was improved when using the more viscous buffer, which represented the reciprocal value of minimum mobility (0.083 cp^{-1}). Fig. 12 shows the production histories for these two runs. Since this minimum mobility value can establish adequate mobility control at very low rates, an improvement in the displacement efficiency was achieved.

However, we are not assuming that unit mobility ratio can be achieved at the higher polymer concentration. This is because of the often-observed increase in polymer solution mobility due to slug/polymer solution interaction.

Sulfonate and Polymer Adsorption

In the micellar flooding process, there can be a loss of miscibility because of either mixing or adsorption of the micellar slug. It is necessary, therefore, to determine if sulfonate adsorption varies substantially with the flood advance rate. Theoretically, if the residence time ($\tau = L/v$) of the micellar slug is long enough (low rates), adsorption on the rock surface may occur.

A series of experiments using a constant weight of crushed Berea sandstone and different concentrations of the micellar solution was carried out to investigate the adsorption of the sulfonate from the micellar solution.

Flasks containing a certain weight of crushed Berea sandstone were used for the experimental work. Micellar solutions (with or without polymer solution) with different concentrations were added to the flasks. All samples were shaken approximately twice a day to keep the micellar sample uniform throughout the flask. Periodically, a 15- to 20-cm^3 sample was taken from each flask. These samples were filtered to remove any sandstone particles. An

*Minimum values obtained from the production data.

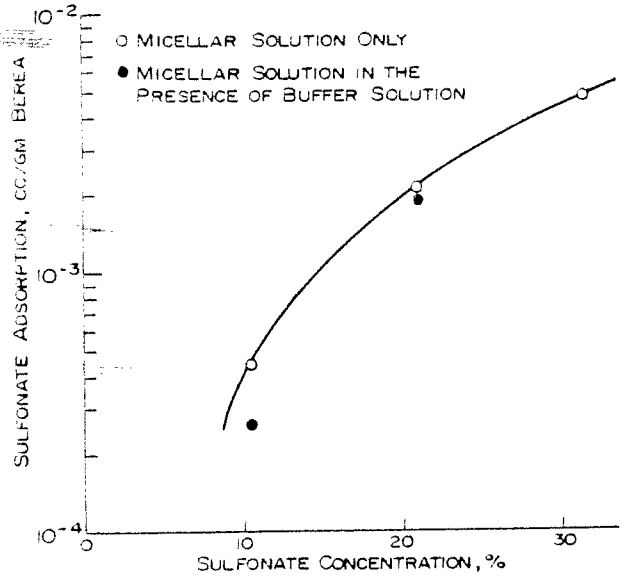

Fig. 13 – Effect of Kelzan buffer on sulfonate adsorption.

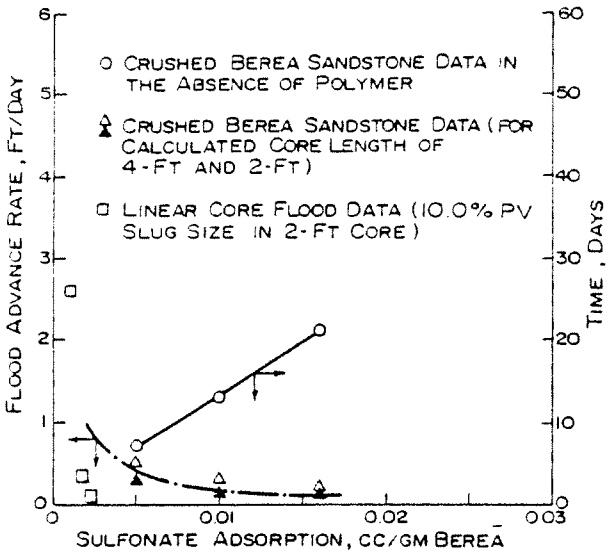

Fig. 14 – Effect of flood advance rate on sulfonate adsorption.

equal amount of a calcium chloride solution was added to each sample to separate the micellar into oleic phase and aqueous phase. The samples were undisturbed overnight to allow time for the two phases to separate. After separations, the oleic phase was analyzed with an infrared spectrophotometer to determine the percent sulfonate in the oleic phase. The percent sulfonate in the oleic phase then was converted to percent sulfonate in the complete micellar solution. This value then was compared with the percent sulfonate in the original micellar solution. The difference in the two values is the percent of the sulfonate adsorbed. Fig. 13 shows the effect of sulfonate concentration as a function of adsorption on the Berea sand, and it is seen that the amount adsorbed increases with concentration. This figure also shows the effect of the presence of the polymer solution on sulfonate adsorption. It should be mentioned that all points appearing in Fig. 13 are average values of 10 experiments carried out under the same conditions. As shown in this figure, less adsorption was obtained in the presence of polymer solution. In addition, this behavior is more significant at the lower sulfonate concentration. The behavior of sulfonate adsorption in the presence of buffer solution (all other factors being unchanged) indicates that some of the polymer was adsorbed on the rock surface. This is true, since polymer adsorption depends on the nature of the rock and the polymer solution. The reduced sulfonate adsorption in the presence of the polymer solution is a desirable phenomenon from the viewpoint of sulfonate conservation and integrity of the micellar slug.

Another series of experiments using crushed Berea sandstone and micellar solutions was carried out to find at what rate sulfonate adsorption occurs. Fig. 14 shows the amount of sulfonate adsorbed on crushed Berea as a function of number of days that the micellar fluid contacts the rock. The crossplot of adsorption as a function of frontal advance rate in the same figure is based on the assumption that 1 PV of the micellar has been injected into the cores. Fig. 14 shows that sulfonate adsorption decreases markedly with frontal advance rate.

Three linear core tests were devoted to study sulfonate adsorption during the micellar flooding process at high and low rates. The data obtained from the core tests showed that the decrease in flow rate caused a small observable change in sulfonate adsorption as shown in Fig. 14. This behavior was due to the presence of the buffer solution used in the core test.

Phase Behavior, Micellar Slug Breakdown, and Mixing Mechanism

The pseudoternary diagram for the micellar slug/crude/brine system was obtained on the basis of phase properties of a large number of samples chosen on the ternary diagram.[12]

Fig. 15 is a ternary diagram of the Richburg-micellar/Bradford-crude/sodium-chloride-brine system. As shown in this diagram, Line XYZ passes from the immiscible region to the small miscible region, crossing the binodal curve at Point Y, when the micellar solution is added to a mixture of oil and water represented by Point X. The ternary diagram, however, indicates that the system used in the present investigation was almost immiscible.

Fig. 16 is a similar diagram for the Bradford-micellar/Bradford-crude/350-ppm-Kelzan-buffer system. In this case, the miscibility region is nearly the same as in the previous system.

The phase behavior of the system used in this study was shown in Figs. 15 and 16 discussed previously. These ternary diagrams indicate that the breakdown of the micellar slug occurs soon after its injection.

Additionally, it was found that tertiary oil recovery at 1 ft/D decreased if the micellar slug was

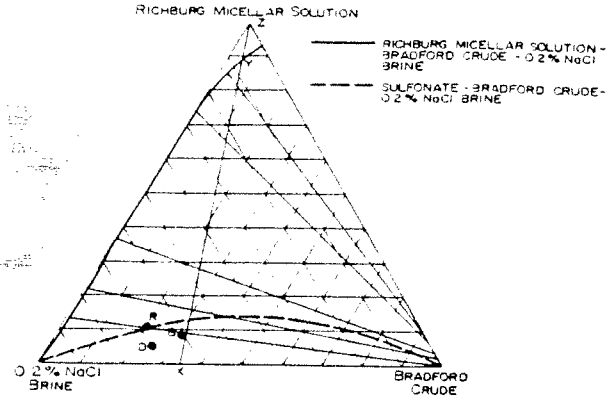

Fig. 15 – Phase diagram of Richburg-micellar/Bradford-crude/0.2%-NaCl-brine system.

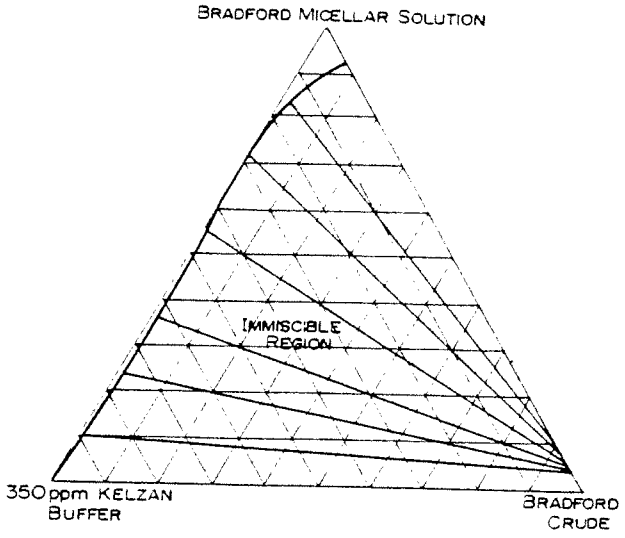

Fig. 16 – Phase diagram of Bradford-micellar-solution/Bradford-crude/350-ppm-Kelzan-buffer system.

decomposed, whereas at 0.5 ft/D the oil recovery showed a slight increase when using the decomposed slug. As mentioned before, this implies similar displacement behavior for both integral and decomposed slugs at 0.5 ft/D.

As mentioned earlier, viscous and capillary forces and mobility control play an important role in the mechanism of the displacement process. In addition to these factors, rate itself may be a factor in the decomposition of the slug. This can be confirmed by Fig. 4 where the tertiary recovery behavior with both integral and decomposed slugs at 1.0 and 0.5 ft/D is shown. Comparison of the two cases shows that the difference in oil recovery for the integral and decomposed slug is significant at 1.0 ft/D, whereas at 0.5 ft/D this difference is negligible. In other words, the micellar slug was affected by the mixing mechanism (decomposition) to an extent that depends on the flood advance rate. Phase behavior of ternary diagram shown in Fig. 15 ensures that the micellar slug in both cases remains in the immiscible region. However, in the case of the sulfonate/Bradford-crude/0.2%-NaCl-brine system, Points R and D (which represent the integral slug and the decomposed slug, respectively) indicate that the composition represented by Point D is in the immiscible region, whereas Point R is on the binodal curve.

Actually, when the slug breakdown theory was proposed, it was expected that the study of this effect will lead to significant conclusions related to the micellar behavior taking place in the core. This is because decomposition of the micellar slug always implies associated changes in sulfonate concentration, viscosity, and interfacial properties.

Since the final oil saturation was reduced by the breakdown of the slug at 1.0 ft/D and since this behavior was not observed at 0.5 ft/D, the slug breakdown took place as a result of changing flood advance rate. Phase behavior of the system used in this study indicates that the breakdown of the micellar slug occurs soon after its injection. This means that the displacement behavior at both rates should be similar. However, the experimental results showed different behavior at 1.0 and 0.5 ft/D. This may be due to the longer contact time at low flood advance rates which permits greater mass transfer between the aqueous and oleic phases. This may have resulted in the regeneration of the slug at lower rates.

Interpretation of Rate Effect in Light of Mechanisms Present

Two principal mechanisms are responsible for high oil recoveries at both high and low rates, thus leading to a minimum in the recovery-rate curve. At high rates, the recovery increase is due to the predominance of viscous forces (high capillary numbers were obtained at these rates), leading to the high values of the pressure gradient observed during the flood. At low rates, recovery tends to decrease with decreasing rate due to the very low pressure gradients (Fig. 6). However, mobility control starts to make itself felt more strongly as the rate decreases. The minimum total mobility of the oil/water bank was found to be 0.083 cp^{-1} on the basis of relative permeability measurements. To obtain a favorable mobility ratio, the mobility of the buffer solution should be less than this minimum value, which can be obtained at very low rates as Fig. 8 shows. At the same time, the variation of the total mobility of the stabilized bank was found to be rate independent, which indicates that the mobility of the buffer solution is the controlling parameter in improving the displacement efficiency at very low flood advance rates. This was verified by carrying out an experimental run at the reciprocal of the minimum mobility (12 cp).

The results of this run (using 470-ppm Kelzan buffer) indicated that the displacement efficiency was

improved as shown in Fig. 12. Hence, this minimum mobility value can establish adequate mobility control at very low rates; thus, an improvement in the displacement efficiency was achieved.

Minimum rate point, which is defined as the flood advance rate at which the tertiary oil recovery was a minimum, was shifted toward the right of the minimum rate point of the 2-ft cores as the core length increased as shown in Figs. 1 and 2. This behavior could be explained in the light of the mechanisms discussed previously. It has been established that the mobility of the Kelzan buffer that moved ahead of the brine was reduced by flow rate. For a given porous medium having the same cross-sectional area and the same injection rate, the pressure difference was higher in the longer cores. This allows the effect of mobility control by the buffer solution to appear early in the 4-ft cores. Therefore, it can be seen that the minimum rate point is shifted toward the right when core length is increased. Actually, what has been said will depend on the system used.

Effect of Rate on Formation of Stabilized Oil/Water Bank

The production histories for the 10% PV slug displacements in 4-ft-long cores at different rates are shown in Fig. 17. Cumulative oil recovery is expressed as a percentage of tertiary oil in place. Production histories for rates of 4.35 and 0.5 ft/D show that there is a wider stabilized oil/water bank (0.43 to 0.57) compared with that for a rate of 0.94 ft/D (0.27). Although at 0.5 ft/D the micellar solution production was small, the oil recovery increased. This could be explained by the low mobility of the buffer at this rate or the much lower interfacial tension inside the core than the externally measured values, which implies an improvement in the displacement efficiency.

It is evident from the production histories for different rates but same slug size and core length that the stabilized oil/water bank breakthrough varies with rate.

This can be explained by the bypassing of the core resident oil and water by the micellar slug front. This observation agreed with what has been published in the literature.[6,10,13]

Implications of Very Low Flood Advance Rates

The Lawry-Penn Grade-DOE project is a field test to demonstrate the efficiency and economics of the tertiary recovery of oil by micellar solutions from a low-permeability (7-md) depleted waterflooded reservoir. The field advance rates in this project are comparable with our laboratory low rates (on the order of 0.10 ft/D). This flood is still in progress, and the response is yet to come.

An understanding of the effect of the flood advance rate will be of value in the design of micellar solutions and mobility buffers. A mechanistic and quantitative basis for interpreting the field test results then could be obtained. In addition, useful correlations of the final oil saturation with rate are now available from the laboratory tests.

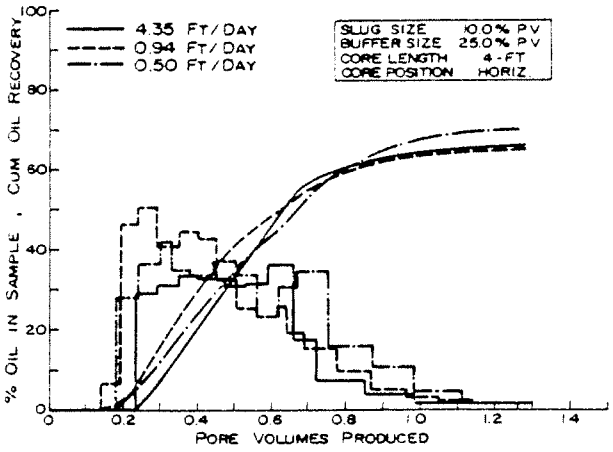

Fig. 17 – Production histories for 10% PV slug displacements in 4-ft cores at different flood advance rates.

Conclusions

Experiments were carried out where micellar slugs used in the Pennsylvania field tests were injected at rates of 0.10 to 5.20 ft/D into waterflooded 2- and 4-ft Berea sandstone cores. The following conclusions can be derived from this work.

1. Oil recovery by micellar solutions was found to be rate dependent for all slug sizes tested.
2. Oil recovery tends to decrease with decreasing rate up to a point; thereafter, it shows a small increase with further decrease in rate.
3. On the basis of the viscosity/shear characteristics of the polymer employed, mobility control by the buffer is rate dependent.
4. Mobility of the buffer solution decreases with decreasing rate.
5. Oil recovery is a function of the ratio between viscous and capillary forces, and it was found that the high value of this ratio was the controlling parameter in increasing the fractional flow of oil in the stabilized bank.
6. Sulfonate adsorption on Berea sandstone increases with solution concentration. For the same concentration, a noticeable change in adsorption was observed for different rates.
7. Reduced sulfonate adsorption was observed on the crushed Berea sandstone under static conditions in the presence of the polymer solution.
8. The stabilized oil/water bank size and its breakthrough time were rate dependent.
9. The micellar slug was affected by its breakdown to an extent that depended on flow rate.

Nomenclature

A = area of core cross section, sq ft
c = parameter found from drop dimensions
d = measured diameter of drop, cm
f = fractional flow, dimensionless
k = absolute permeability, darcy

TABLE 2 – PROPERTIES OF POROUS MEDIA

Type	Core Length (ft)	Core Diameter (in.)	Porosity (%)	Permeability (md)
Berea sandstone (Core A)	4	2	20	107 to 332
Berea sandstone (Core B)	2	2	20	71 to 239

TABLE 3 – COMPOSITION OF MICELLAR SOLUTIONS

Component	Composition (vol%)
Richburg micellar slug	
Water	68.03
Diesel oil	17.97
Sulfonate TRS 16*	5.46
Sulfonate TRS 40*	5.51
Amyl alcohol	2.37
Butyl alcohol	0.66
Bradford micellar slug	
Water	59.65
Sulfonate TRS 16	4.04
Sulfonate TRS 48*	4.92
Crude oil	27.58
Neodahl	0.87
Amyl alcohol	1.30
n-butyl alcohol	1.64

*Witco Chemical Co., Bradford, PA.

TABLE 4 – PHYSICAL PROPERTIES OF LIQUIDS

Liquid	Viscosity (cp)	Specific Gravity	Refractive Index
Bradford crude	3.4	0.794	1.454
Richburg slug	11.8	0.968	1.368
Bradford slug	7.0	0.809	1.370
2% NaCl brine	1.02	1.010	1.332
350-ppm Kelzan buffer	5.0 to 6.0	1.00	1.3325

k_r = relative permeability, dimensionless
K = constant
L = length of core, ft
n = Ostwald-de Waele power law index
N_c = capillary number, dimensionless
$\bar{p}$ = tensiometer period read off counter, ms/RRV
Δp = pressure difference, psi
R_F = flow resistance
t = time variable, days
v = frontal velocity, ft/D
w = speed of revolution radius, rad/s
γ = interfacial tension, dyne/cm
$\dot{\gamma}$ = shear rate, seconds^{-1}
λ = mobility, cp^{-1}
μ = viscosity, cp
$\Delta\rho$ = density difference between the two phases, g/cm^3
ϕ = porosity, dimensionless

Subscripts

b = stabilized bank
o = oil or oleic
p = polymer solution
t = total
w = water or aqueous

Acknowledgment

This investigation was supported by the U.S. DOE under Contract No. E(40-1)-5078.

References

1. Gogarty, W.B. and Tosch, W.C.: "Miscible-Type Waterflooding: Oil Recovery With Micellar Solutions," *J. Pet. Tech.* (Dec. 1968) 1407-1414; *Trans.*, AIME, **243.**
2. Davis, J.A. Jr. and Jones, S.C.: "Displacement Mechanisms of Micellar Solutions," *J. Pet. Tech.* (Dec. 1968) 1415-1428; *Trans.*, AIME, **243.**
3. Bleakley, E.B.: "How Maraflood Process Performs," *Oil and Gas J.* (Nov. 29, 1971).
4. Taber, J.J., Kamath, I.S.K., and Reed, R.: "Mechanism of Alcohol Displacement of Oil from Porous Media," *Soc. Pet. Eng. J.* (Sept. 1961) 195-212; *Trans.*, AIME, **209**; *Miscible Processes*, Reprint Series, SPE, Dallas (1965) **8**, 39-56.
5. Taber, J.J. and Meyer, W.K.: "Investigations of Miscible Displacements of Aqueous and Oleic Phases From Porous Media," *Soc. Pet. Eng. J.* (March 1964) 37-48; *Trans.*, AIME, **231**; *Miscible Processes*, Reprint Series, SPE, Dallas (1965) **8**, 57-68.
6. Healy, R.N., Reed, R., and Carpenter, C.W.: "A Laboratory Study of Microemulsion Flooding," *Soc. Pet. Eng. J.* (Feb. 1975) 87-100; *Trans.*, AIME, **259.**
7. Sayyouh, M.H., Farouq Ali, S.M., and Stahl, C.D.: "Effect of Frontal Advance Rate on Oil Recovery by Micellar-Polymer Displacement," paper presented at ERDA Third Symposium on Enhanced Oil and Gas Recovery, Tulsa, Aug. 1977.
8. Morrow, N.R.: "Interplay of Capillary, Viscous and Buoyancy Forces in the Mobilization of Residual Oil," Paper 78-29-24, Petroleum Soc., CIM.
9. Taber, J.J.: "Dynamic and Static Forces Required to Remove a Discontinuous Oil Phase From Porous Media Containing Both Oil and Water," *Soc. Pet. Eng. J.* (March 1969) 3-12.
10. Sayyouh, M.H.: "Theoretical and Experimental Studies on Rate Effects in Micellar Displacement in Sandstone Cores," PhD thesis, Pennsylvania State U., University Park (1979).
11. Chang, H.L., Al-Rikabi, H.H., and Pusch, W.: "Determination of Oil/Water Bank Mobility in Micellar-Polymer Flooding," *J. Pet. Tech.* (July 1978) 1055-1060.
12. Mohyiddin, M.S.: "Phase Behavior of Micellar Solution-Bradford Crude-Water System and Its Mathematical Representation," MS thesis, Pennsylvania State U., University Park (Aug. 1978).
13. Sandrea, R. and Stahl, C.D.: "Considerations in the Recovery of Bradford Crude by Composite Solvent Slugs," *Soc. Pet. Eng. J.* (March 1965) 45-50; *Trans.*, AIME, **234.**
14. Wade, W.H., Schechter, R.S., Morgan, J.C., and Jacobson, J.K.: "Low Interfacial Tensions Involving Mixtures of Surfactants," *Soc. Pet. Eng. J.* (April 1977) 122-128.
15. Unsal, E., Duda, J.L., Klaus, E.E., and Liu, H.T.: "Solution Properties of Mobility Control Polymers," paper SPE 6625 presented at the SPE 1977 Eastern Regional Meeting, Pittsburgh, Oct. 26-28, 1977.
16. Dabbous, M.: "Displacement of Polymers in Waterflooded Porous Media and Its Effects on a Subsequent Micellar Flood," *Soc. Pet. Eng. J.* (Oct. 1977) 358-368; *Trans.*, AIME, **263.**

APPENDIX A
Material, Apparatus, and Experimental Techniques

The properties of the porous medium used in the experimental investigation are given in Table 2. The micellar solutions being used in the Pennsylvania field tests were employed for this work. These micellar solutions are referred to as the Richburg and Bradford slugs. The compositions of the two micellar solutions are shown in Table 3. The mobility buffer

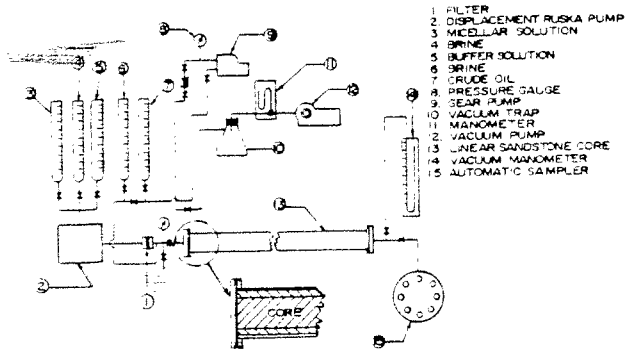

Fig. 18 – Experimental apparatus.

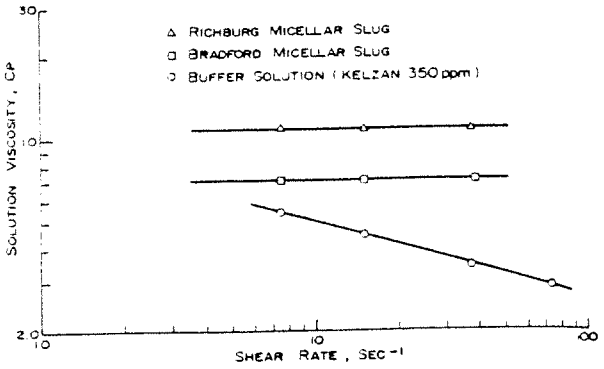

Fig. 19 – Rheological behavior of micellar solutions and Kelzan buffer (350 ppm).

consists of 350-ppm Kelzan. The physical properties of the different fluids used in this research are shown in Table 4.

The experimental apparatus is shown schematically in Fig. 18. The sandstone cores initially were saturated with 2% sodium chloride brine, then flooded with crude, and thereafter waterflooded with brine. The core then attained the residual oil saturation, and a tertiary micellar flood then could be initiated. A new core was used for each run. The same brine was used for driving the mobility buffer.

The method used in finding the interfacial tension was the spinning drop technique[14] based on measuring the length L and width h of the drop. If $0 \le L-h < 3h$, the following equation was used.[14]

$$\gamma = \frac{\Delta\rho\, w^2}{4C} \quad \ldots\ldots\ldots\ldots\ldots\ldots\ldots\ldots\ldots\ldots (A\text{-}1)$$

On the other hand, if the drop length was greater than four times the width (i.e., $L > 4h$), the interfacial tension was determined by[14]

$$\gamma = 5.2203 \times 10^5 \frac{\Delta\rho d^3}{p^{-2}} \quad \ldots\ldots\ldots\ldots\ldots\ldots\ldots\ldots (A\text{-}2)$$

Rheological Behavior of Micellar Solutions and Mobility Buffers

The micellar solutions used exhibited the rheological behavior of a Newtonian fluid shown in Fig. 19. The viscous properties of the Kelzan buffer as measured at room temperature in a Brookfield viscometer are shown in the same figure. The laboratory tests showed that the viscosity of the mobility buffer decreases with mechanical shear.

APPENDIX B
Mobility of Buffer Solution

The total mobility of the stabilized oil/water bank is defined as

$$\lambda_t = \lambda_o + \lambda_w = \frac{k_{ro}}{\mu_o} + \frac{k_{rw}}{\mu_w} \quad \ldots\ldots\ldots\ldots\ldots\ldots\ldots\ldots (B\text{-}1)$$

The mobility ratio between the buffer bank and the stabilized bank can be written as

$$M = \frac{k_p}{\mu_p}\left(\frac{k_{ro}}{\mu_o} + \frac{k_{rw}}{\mu_w}\right)^{-1} \quad \ldots\ldots\ldots\ldots\ldots\ldots\ldots\ldots (B\text{-}2)$$

or

$$M = \frac{k_p}{\mu_p} \cdot R_F \quad \ldots\ldots\ldots\ldots\ldots\ldots\ldots\ldots\ldots\ldots (B\text{-}3)$$

where R_F is the flow resistance.

To obtain adequate mobility, the mobility of the buffer bank displacing the micellar slug must be equal to or less than the total mobility of the oil/water bank – i.e.,

$$\left(\frac{k_p}{\mu_p}\right) R_F \le 1 \quad \ldots\ldots\ldots\ldots\ldots\ldots\ldots\ldots\ldots\ldots (B\text{-}4)$$

Fig. 19 shows that the buffer solution exhibits non-Newtonian behavior. The relationship between the apparent viscosity of the buffer solution and shear rate can be obtained as

$$\mu_p = \bar{K}(\dot{\gamma})^{n-1} \quad \ldots\ldots\ldots\ldots\ldots\ldots\ldots\ldots\ldots\ldots (B\text{-}5)$$

To calculate the shear rates in a reservoir, the following equation can be used.[15]

$$\dot{\gamma} = \frac{3v\left(3+\frac{1}{n}\right)}{\sqrt{150\,\bar{K}\phi}}, \quad \ldots\ldots\ldots\ldots\ldots\ldots\ldots\ldots (B\text{-}6)$$

where the power law index n can be obtained from Fig. 19.

Finally, mobility of the buffer solution during a displacement process can be evaluated from Eqs. B-5 and B-6 as follows.

$$\lambda_p = \frac{k}{\bar{K}}\left[\frac{3v\left(3+\frac{1}{n}\right)}{\sqrt{150\,\bar{K}\phi}}\right]^{1-n}, \quad \ldots\ldots\ldots\ldots (B\text{-}7)$$

or

$$\lambda_p = \frac{k}{\bar{K}}\left[\frac{v\left(3+\frac{1}{n}\right)}{\sqrt{16.67\,\bar{K}\phi}}\right]^{1-n}, \quad \ldots\ldots\ldots\ldots (B\text{-}8)$$

SI Metric Conversion Factors

cp	× 1.0*	E−03	= Pa·s
dyne/cm	× 1		= mN/m
ft	× 3.048*	E−01	= m
in.	× 2.54*	E+00	= cm
psi	× 6.894 757	E+00	= kPa
sq ft	× 9.290 304*	E−02	= m^2

*Conversion factor is exact.

SPEJ

Original manuscript received in Society of Petroleum Engineers office May 1, 1978. Revised manuscript received June 9, 1981. Paper accepted for publication June 16, 1981. Paper (SPE 7639) first presented at the SPE 1978 Eastern Regional Meeting, held in Washington, DC, Nov. 1-3.

Phase Behavior of CO_2 and Crude Oil in Low-Temperature Reservoirs

F.M. Orr Jr., SPE, New Mexico Inst. of Mining and Technology
A.D. Yu,* SPE, New Mexico Inst. of Mining and Technology
C.L. Lien, SPE, New Mexico Inst. of Mining and Technology

Abstract

Phase behavior of CO_2/crude-oil mixtures which exhibit liquid/liquid (L/L) and liquid/liquid/vapor (L/L/V) equilibria is examined. Results of single-contact phase behavior experiments for CO_2/separator-oil mixtures are reported. Experimental results are interpreted using pseudoternary phase diagrams based on a review of phase behavior data for binary and ternary mixtures of CO_2 with alkanes. Implications for the displacement process of L/L/V phase behavior are examined using a one-dimensional finite difference simulator. Results of the analysis suggest that L/L and L/L/V equilibria will occur for CO_2/crude-oil mixtures at temperatures below about 120°F (49°C) and that development of miscibility occurs by extraction of hydrocarbons from the oil into a CO_2-rich liquid phase in such systems.

Introduction

The efficiency of a displacement of oil by CO_2 depends on a variety of factors, including phase behavior of CO_2/crude-oil mixtures generated during the displacement, densities and viscosities of the phases present, relative permeabilities to individual phases, and a host of additional complications such as dispersion, viscous fingering, reservoir heterogeneities, and layering. It generally is acknowledged that phase behavior and attendant compositional effects on fluid properties strongly influence local displacement efficiency,[1-5] though it also is clear that on a reservoir scale, poor vertical and areal sweep efficiency (caused by the low viscosity of the displacing CO_2) may negate the favorable effects of phase behavior.[3]

Interpretation of the effects of phase behavior on displacement efficiency is made difficult by the complexity of the behavior of CO_2/crude-oil mixtures. The standard interpretation of CO_2 flooding phase behavior, given first by Rathmell *et al.*[1] is that CO_2 flooding behaves much like a vaporizing gas drive, as described originally by Hutchinson and Braun.[6] During a flood, vapor-phase CO_2 mixes with oil in place and extracts light and intermediate hydrocarbons. After multiple contacts, the CO_2-rich phase vaporizes enough hydrocarbons to develop a composition that can displace oil efficiently, if not miscibly. The picture presented by Rathmell *et al.*[1] appears to be consistent with phase behavior observed for CO_2/crude-oil mixtures as long as the reservoir temperature is high enough. Table 1 summarizes data reported for CO_2/crude-oil mixtures. Of the 10 systems studied, all those at temperatures above 120°F (50°C) show only L/V equilibria while those below 120°F exhibit L/L/V separations (Stalkup[3] also reports two phase diagrams that are qualitatively similar to the other low-temperature diagrams but does not give temperatures). Thus, at temperatures not too far above the critical temperature of CO_2 [88°F (31°C)], mixtures of CO_2 and crude oil exhibit multiple liquid phases, and at some pressures L/L/V equilibria are observed.[5,7,8]

It has not been established whether Rathmell *et al.*'s[1] interpretation of the process mechanism can be extended to cover the more complex phase behavior of low-temperature CO_2/crude-oil mixtures. In a recent paper, Metcalfe and Yarborough[4] argued that low-temperature CO_2 floods behave more like condensing gas drives,[6] whereas Kamath *et al.*[13] concluded that an increase in the solubility of liquid-phase CO_2 in crude oil at temperatures near the critical temperature of CO_2 should cause more efficient displacements of oil by CO_2. Huang and

*Now with Texaco Inc.

0197-7520/81/0008-8813$00.25